environments

Article

Concentrations and Oxidative Potential of $PM_{2.5}$ and Black Carbon Inhalation Doses at US–Mexico Port of Entry

Rita Zurita [1], Penelope J. E. Quintana [2], Yanis Toledano-Magaña [3], Fernando T. Wakida [1], Lupita D. Montoya [2] and Javier Emmanuel Castillo [1,*]

[1] Facultad de Ciencias Químicas e Ingeniería, Universidad Autónoma de Baja California, Calzada Universidad 14418 Parque Industrial Internacional, Tijuana 22427, Mexico; rita.zurita@uabc.edu.mx (R.Z.); fwakida@uabc.edu.mx (F.T.W.)
[2] School of Public Health, San Diego State University, 5500 Campanile Drive, San Diego, CA 92182-4162, USA; jquintan@sdsu.edu (P.J.E.Q.); ldmontoya@sdsu.edu (L.D.M.)
[3] Nanoscience and Nanotechnology Center (CNyN), Campus Ensenada, National Autonomous University of Mexico (UNAM), Mexico City 04510, Mexico; yanis.toledano@uabc.edu.mx
* Correspondence: castillo@uabc.edu.mx; Tel.: +52-664-979-75-00 (ext. 54312)

Abstract: Located between Mexico and the US, the San Ysidro/El Chaparral Land Port of Entry (SYPOE) is one of the busiest border crossings in the world. People with activities at the SYPOE are exposed to vehicular pollutants, especially particles with aerodynamic diameters < 2.5 µm ($PM_{2.5}$) and black carbon (BC), both associated with adverse health effects. This study presents the first $PM_{2.5}$ and BC concentration measurements collected on the Mexican side of the SYPOE. The oxidative potential (OP) for $PM_{2.5}$ and the inhalation dose of BC for people at the border were also evaluated. Autumn and winter showed the highest $PM_{2.5}$ concentrations (at 28.7 µg m^{-3} and 28.2 µg m^{-3}, respectively). BC concentration peaked in the winter of 2017 (at 5.7 ± 6 µgm^{-3}), demonstrating an increase during periods with low wind speeds. The highest OP_{DTT} of $PM_{2.5}$ was reached in winter, with a value of 18.5 pmol min^{-1} μg^{-1} (0.6 nmol $min^{-1}m^{-3}$). The highest average daily inhalation dose for pedestrians was registered in the autumn of 2018 (5.9 µg for a 60-min waiting time), whereas, for workers, it was in the winter of 2017 (19 µg for a 10-h shift on average). Decreasing waiting times for pedestrians and adjusting work schedules for border workers on high concentration days could ameliorate environmental justice.

Keywords: workers; fine particle matter; san ysidro land port of entry; traffic pollution; pedestrians; oxidative potential

Citation: Zurita, R.; Quintana, P.J.E.; Toledano-Magaña, Y.; Wakida, F.T.; Montoya, L.D.; Castillo, J.E. Concentrations and Oxidative Potential of $PM_{2.5}$ and Black Carbon Inhalation Doses at US–Mexico Port of Entry. *Environments* **2024**, *11*, 128. https://doi.org/10.3390/environments11060128

Academic Editors: Sripriya Nannu Shankar, Tara Sabo-Attwood, Jana S. Kesavan and Sanghee Han

Received: 8 May 2024
Revised: 14 June 2024
Accepted: 16 June 2024
Published: 18 June 2024

1. Introduction

The US–Mexico border is a unique region, with shared water resources and atmospheric basins. This joint border area has a complex relationship encompassing social, cultural, and economic elements. The urban population in this area has been growing in the last decade, with growth rates currently higher than national ones. From 1969 to 2020, the growth rate exceeded 60% on both sides of the border [1,2]; however, this growth has not included infrastructure improvements, generating binational environmental and public health challenges [3,4]. As such, the community of San Ysidro has been recently classified as a priority area in terms of environmental justice by the state of California [5].

The San Ysidro/El Chaparral Port of Entry (SYPOE) is the most active ports in the western hemisphere. The El Chaparral Port of Entry is operated by the Mexican Customs Authority for vehicles and pedestrians crossing from the United States into Mexico, while the San Ysidro Port corresponds to the US Customs Authority for entering the US [6]. In 2017, approximately 70,000 passenger vehicles and 20,000 pedestrians crossed the border into San Ysidro per day [7]. In 2019, waiting times reached up to 3 h [6].

Nearby workers, border crossers, and communities are exposed to harmful air pollutants due to the constant emissions from heavy-duty diesel trucks and passenger vehicles at the US–Mexico Ports of Entry. Previous studies have associated high concentrations of ultrafine particles, carbon monoxide (CO), and black carbon (BC) with waiting times during border crossing [4,8]. People near this area might also be exposed to pollutants from vehicles waiting to cross [9]. A study at the SYPOE found two-fold increases in exposure to $PM_{2.5}$ for pedestrian crossers compared to those of people who work, study, or live in San Ysidro but do not cross into Mexico [8]. In addition, Mukherjee et al. have shown a change in $PM_{2.5}$ concentration and road distances, and Karner et al. found that $PM_{2.5}$ decreased 10–50% at 400 m from roadways in the US [10,11].

Epidemiological studies have indicated adverse effects of air pollution related to traffic, including the development of respiratory diseases [12] and cardiovascular diseases [13], among others [14]. PM may contain BC, which has been used as an indicator of diesel combustion, as well as trace metals, quinones, and other compounds [15,16]. Roadway PM may generate reactive oxygen species (ROS), leading to oxidative stress [17]. The capacity of PM to generate ROS is referred to as oxidative potential (OP) and is influenced by factors such as PM size and chemical composition [18]. There are several acellular methods to determine OP in PM. One of the most commonly used methods is the dithiothreitol assay (DTT), which has been used to demonstrate the correlations with asthma decreases in microvascular function [19], congestive heart failure [20], and ischemic heart disease [21]. Therefore, oxidative potential measured via DTT (OP_{DTT}) can indicate possible health consequences derived from $PM_{2.5}$ [18]. Similarly, BC has been evidenced to be a better air quality indicator to evaluate the health risks as a result of an air quality dominated by primary combustion particles [22].

Other studies on border air pollution and related health problems [23] have yielded recommendations for programs to reduce air pollution at border crossings [24,25]. The objective of this study was to measure $PM_{2.5}$ concentrations and their associated OP at the SYPOE. BC concentrations were also measured, and the resulting inhalation doses of border crossers and workers at the SYPOE were determined. This is the first study that reports the OP associated with $PM_{2.5}$ and the BC inhalation dose at a border crossing between the US and Mexico. The results presented herein could inform decision-makers about exposure levels at the SYPOE, as well as about strategies to reduce these levels in favor of the benefit of nearby workers, border crossers, and communities.

2. Materials and Methods

2.1. Air Sampling Sites

Figure 1 shows the general location of this study. The San Diego Air Pollution Control District Donovan Site, M1, (32°34′41.4″ N, 116°55′16.9″ W) is located near the Richard J. Donovan Correctional Facility. It is situated about 3.9 km southwest of the Otay Mesa Port of Entry (OMPOE) and 10 km northeast of the SYPOE. The local vehicular flow is composed mostly of diesel trucks.

Site M2 is part of the air quality monitoring network of Baja California, Mexico (32°29′51.06″ N, 116°58′37.34″ W). It is located 7 km southeast of the SYPOE, in a school within a populated area of Tijuana, surrounded by local roads with continuous vehicular flow. Sites M1 and M2 present an overview of the air quality in the United States and Mexico.

Site M3 is located in Tijuana, B.C., Mexico (32°32′28″ N, 117°01′36″ W), 200 m southeast of the SYPOE, close to the pedestrian crossing line and the Secure Electronic Network for Travelers Rapid Inspection System (SENTRI) line (Figure 1).

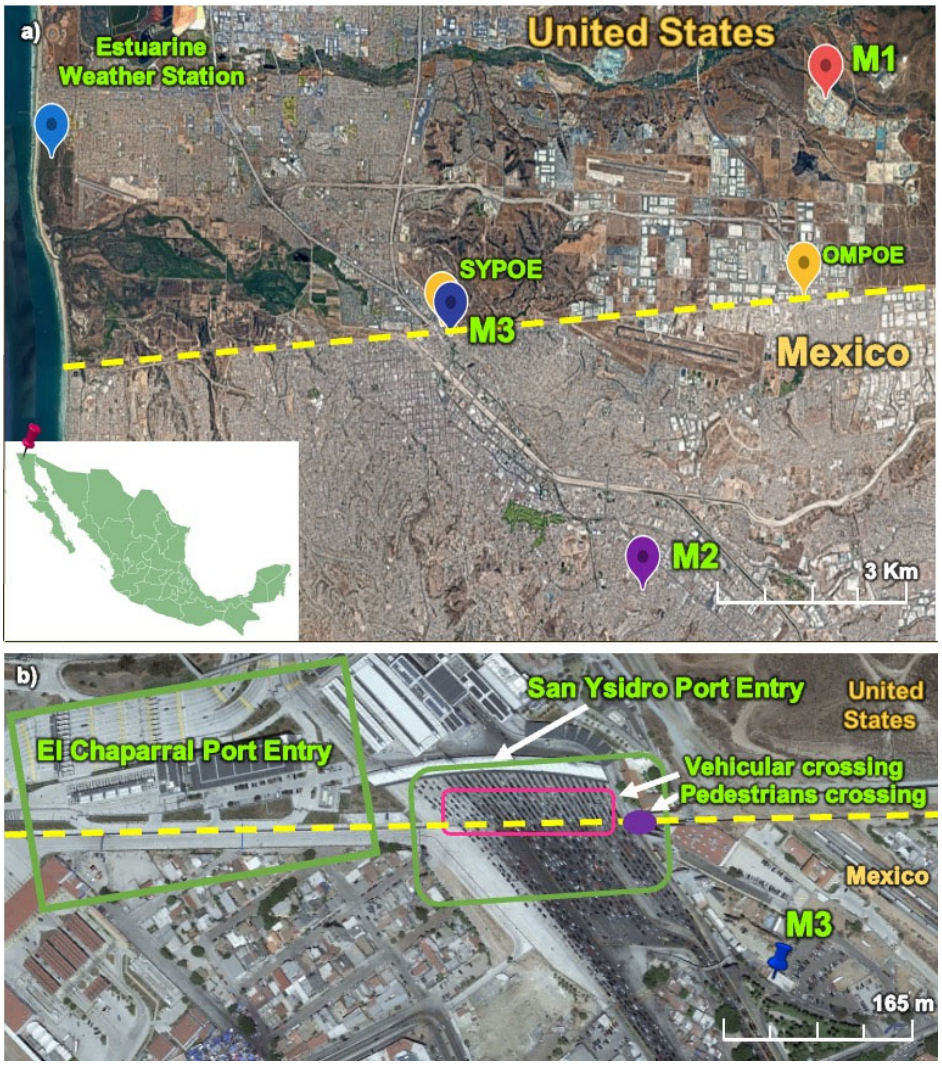

Figure 1. Location of study (insert: location of Tijuana on the map of Mexico): (**a**) regional level including the three sampling sites (M1, M2, M3), SYPOE, OMPOE and the Estuarine Weather Station. (**b**) Local level, including SYPOE and M3. The green rectangles delineate the boundaries of the El Chaparral (large, left) and the San Ysidro (small, right) Ports of Entry. The dashed yellow line represents the international border. The purple oval represents a pedestrian crossing, and the pink rectangle represents a vehicular crossing. Map source: Google Earth.

The air sampler was placed on the balcony on the second floor of a building, about 4 m off the ground. It was decided to set up the equipment in this area for security reasons (to prevent it from being stolen) and because power was available. Both lines to cross the border, vehicular and pedestrian, often pass in front of the first floor of site M3. There were several parking lots and a railway track to the northeast of site M3, about 50 m and 150 m away, respectively. Likewise, many other parking lots and buildings were under construction about 210 m and 600 m to the southeast, respectively. On the southwest, there were vehicular traffic areas (about 300–600 m away) along with the inspection area for the El Chaparral POE (about 670 m away). Finally, a residential area was settled to the east of the SYPOE, whereas a commercial area was located to the west.

2.2. Study Groups

Two groups of people were included in this study: pedestrians crossing the border and local vendors working between the cars in line to cross the border. The first group was considered during the evaluation of exposure and doses of inhaled pollutants during

the waiting periods for crossing the border; there is no information on the number of pedestrians crossing, only information on waiting times. The second group, the workers, were surveyed to assess their long-term exposure due to their occupation.

2.3. Surveys

A short survey consisting of four questions was conducted on fifty local vendors who worked among cars waiting to cross the border. These workers were in closer proximity to the vehicles, compared to the pedestrians crossing the border, and thus more likely to be exposed to higher pollution levels. The short survey included questions about age, work schedule, and number of years in that job. The survey was approved by the Ethics Committee of the College of Chemical Sciences and Engineering at the Autonomous University of Baja California (UABC). The survey was administered a few days after the sampling, during a workday, and it took workers approximately 5 min to complete the survey.

2.4. Sampling Periods, Meteorological Data, and Waiting Time

$PM_{2.5}$ sampling was conducted from June 2018 to January 2019, and BC sampling was conducted between November 2017 and January 2019. $PM_{2.5}$ and BC sampling was carried out simultaneously during the common days. The detailed data collection schedule is provided in Table S1. Sampling was carried out continuously for periods of two weeks at a time. Sufficient air sampling was performed to ensure at least two samples per day of the week were collected.

Hourly data on temperature, relative humidity percentage, wind direction, and wind speed were obtained for the sampling periods reported here. Meteorological data used in this research were retrieved from the website http://www.nerrsdata.org (accessed on 2 October 2020) [26]. Detailed data are provided in Table S2. The weather station was located 4.18 km northwest, at the Tijuana River National Estuarine Research Reserve (coordinates 32°34′28.5″ N, 117°07′37.3″ W), approximately 10 km northwest of M3. The data from the estuary were used since other meteorological stations provided incomplete data for the sampling periods; however, a comparison was made out of the available days to verify that did not differ much. Wind roses were generated using AERMOD View (Version 6.2).

The US Customs and Border Protection (CBP) estimates and publishes on their website (https://bwt.cbp.gov/details/09250401/POV, accessed on 2 October 2020) hourly waiting times for vehicles and pedestrians crossing the border, but they are not archived. The University of Washington created a software program to archive these data, which are available upon request.

2.5. $PM_{2.5}$

$PM_{2.5}$ concentrations from site M1 were attained from the California Air Resources Board, US (https://www.arb.ca.gov, accessed on 2 October 2020), and averaged over the same collection time (3:00 p.m. and ending at 2:30 p.m. $\pm$ 30 min). This schedule was used to collect consecutive samplings and to change the filters of both pieces of equipment at the same time. Moreover, for security and access reasons, entry to site M3 was only allowed in the afternoon. The $PM_{2.5}$ data from site M2 were provided by the Air Quality Network of the Secretaría de Protección al Ambiente of Baja California, Mexico. Data from both sites were collected using a beta attenuation equipment method (BAM), which is considered equivalent to the high-volume sampler according to PROY-NMX-AA-177-SCFI-2015 [27].

$PM_{2.5}$ concentrations at site M3 were collected using a high-volume sampler (TISCH TE-6070, Ohio, US) with an inlet head for $PM_{2.5}$ (TISCH TE-6001, Hamilton, OH, USA). Quartz filters (8 $\times$ 10 Whatman Cat No. 1851-865) were first heat-treated using a furnace (Watlow 935 A, Winona, MN, USA) at 450 °C for 6 h to eliminate organic residues. The filters were loaded onto the sampler and operated at flow rates between 1.12 and 1.18 m^3 min^{-1} [28]. Air samples were collected for 23.5 h, from 3:00 p.m. to 2:30 p.m. $\pm$ 30 min. The filters were removed from the sampler, placed in aluminum foil inside an airtight plastic bag, and

stored at −18 °C (Polar, CH-011, Valencia, Spain). Two field filter blanks were used for each sampling season. Before and after sampling, filters were conditioned at 23 °C and 35% RH. $PM_{2.5}$ masses were determined gravimetrically with an analytical balance (Ohaus Voyager Pro, Model VP114CN, Uster, Switzerland) following the published Standard Operating Procedure MDL016 [29].

2.6. Black Carbon

BC monitoring was carried out using a portable micro aethalometer (Aeth Labs, AE51, San Francisco, CA, USA) at a 100 mL/min flow rate and a sampling rate of 1 min. Viana et al. showed that AE-51 has agreement with the Thermo Multi-Angle Absorption Photometer > 0.8, with differences of 7–12%. The filters were changed every 23.5 h. Optimized noise-reduction averaging (ONA) was applied to reduce fluctuations in the data, which may occur at high sampling rates (i.e., <1 min) [30]. Additionally, the equation presented by Virkkula et al. was used to reduce the effect of the gradual increase of attenuation (ATN) from one sampling period to the next due to the gradual accumulation of optically absorbent particles [31].

2.7. Oxidative Potential

A dithiothreitol (DTT) assay was used to evaluate the oxidative potential of $PM_{2.5}$. A (1/28) section of each filter was cut and then extracted using 15 mL of nanopure water via sonication for 30 min; extracts were filtered using membranes that were 47 mm in diameter with 0.45 µm micropores (Cole-Parmer, SC0407, Lake, IL, USA) [32]. Next, 3 mL of DTT (100 µM in a 0.1 M phosphate buffer, pH 7.9) was placed in a test tube and 100 µL of a PM suspension of a known concentration was added and allowed to react. Then, 0.5 mL aliquots were taken at 5, 10, 15, and 20 min after the reaction commenced [33]. Aliquots were transferred to test tubes with 0.5 mL of 10% trichloroacetic acid to stop the reaction. When all aliquots were inactivated, 50 µL of 5,5′-dithio-bis-(2-nitrobenzoic acid) (DTNB) at 10 mM was added, followed by 2 mL of Tris-base with ethylenediaminetetraacetic acid (EDTA, 0.4 M, pH 8.9), and was then allowed to react for 5 min. The 2-nitro-5-thiobenzoic acid (TNB) formed was quantified with a UV-vis spectrophotometer (Perkin Elmer, Lambda 3A, Waltham, MA, USA) at a wavelength of 412 nm. The samples were run in triplicate (coefficients of variation < 10%). A positive control (9,10-Phenanthrenoquinone, 0.050 µM) and blank (nanopure water), in triplicate, were also included in each test.

The OP_{DTT} was normalized by the collected mass from the filter (OP_{DTTm}) to represent the inherent activity of the PM linked to sources, and by volume (OP_{DTTv}) to characterize the aerosol exposure [34].

2.8. BC Inhalation Dose

The inhalation dose of BC was calculated according to Equation (1) [35], which assumes 100% uptake:

$$D = Cp\ IR\ \Delta t, \quad (1)$$

where D represents the average inhalation dose (µg), Cp is the average BC concentration at a specified microenvironment and time (µg m^{-3}), IR is the inhalation rate ($m^3\ h^{-1}$), and Δt indicates the time of exposure to the pollutant.

BC inhalation doses were calculated for the two distinct groups in this research. The Δt was the time (h) spent by the pedestrians waiting in line to cross the SYPOE in a northbound direction. The second group, the workers, was based on the results of the conducted survey. It should be noted that multiple factors that can influence the IR, such as age, activity level, and gender, among others. In this study, two IR values (published by the US Environmental Protection Agency, EPA) were used: (a) 0.51 $m^3\ h^{-1}$ for an average adult performing light activities (walking, for instance), and (b) 0.78 $m^3\ h^{-1}$, for outdoor workers performing essential income-related activities [36]. The dose for pedestrians was calculated for a period corresponding to the 95th percentile of the seasonal pedestrian waiting time between 4:00 a.m. and 9:00 a.m., which is an interval where people go to work and there is diurnal

variation. The inhalation dose for the workers was calculated individually hour by hour during the working hours.

2.9. Statistical Analysis

The statistical analyses were performed using Statistical Package for Social Sciences (SPSS), version 24. Concentrations of $PM_{2.5}$ and BC were analyzed by non-parametric statistical analysis. Summary statistics were based on daily and 1-h average concentrations of $PM_{2.5}$ and BC, respectively. For these calculations, the vehicular waiting times, temperature, relative humidity (RH), and wind speed were documented using the same periods as the pollutants.

$PM_{2.5}$ concentrations were compared among sites using a Kruskal–Wallis test. Pairwise Mann–Whitney tests were used to compare BC concentrations between seasons and weekdays (Monday to Thursday) versus weekends (Friday to Sunday). Subsequently, the correlations of pollutant concentration with meteorological (temperature, RH, wind speed, and rainfall) data and vehicular waiting time were determined using a Spearman rank analysis. Correlations between BC concentrations and wind speeds (for low and other wind speeds) were also determined [4]. For all analyses, values with $p < 0.05$ were considered relevant.

3. Results and Discussion

3.1. Survey Results

The survey was applied to fifty workers with a 100% completion rate, and the results are presented in Table S4. Seventy-six percent (76%) of the workers reported starting their work shift between 7 a.m. and 10 a.m., and 64% ending it between 7 p.m. and 9 p.m. The respondents stated to be between 15 and 65 years old (median of 36 years), their work-days were around 7 to 14 h long (median of 10 h), and the time they had been working at that job ranged from 1 month to 50 years (median of 7 years).

3.2. Spatial and Temporal Variability of $PM_{2.5}$

Table 1 shows descriptive statistics for $PM_{2.5}$ for the sites and seasons included in this study. Data from the US reference site (M1) and the MX reference site (M2) were compared to the SYPOE (M3). The median $PM_{2.5}$ concentrations measured at M3 were twice as those of M1 in autumn and winter, but not different in summer ($p < 0.05$).

The concentrations of $PM_{2.5}$ at site M3 were higher than site M2 by 30% and 10% in winter and autumn, respectively, but not statistically different; concentrations at site M2 were likely the result of contributions from local sources, as well. In Tijuana, about 80% of the circulating private vehicles are imported from the United States and around 65% are models from the year 2000 and older [37]. Older vehicles tend to increase $PM_{2.5}$ emission estimates [38] and the residents might be exposed to these increased emissions.

The median $PM_{2.5}$ daily concentration at site M3 for the entire campaign was 19.4 $\mu g\ m^{-3}$, comparable to the value of 15 $\mu g\ m^{-3}$ determined by Galaviz et al. near the SYPOE in 2010 [8]. These data are comparable to those determined by a study at the border cities of Nogales, Mexico, and Nogales, Arizona [39]. In that study, the median $PM_{2.5}$ daily concentrations of two sites on the Mexican side were 17.92 and 11.67 $\mu g\ m^{-3}$, and for the two sites on the US side they were 7.23 and 12.05 $\mu g\ m^{-3}$.

Figure 2 shows the time series of 24-h $PM_{2.5}$ concentrations measured near the SYPOE (M3). These concentrations exceeded the 24-h guideline (15 $\mu g\ m^{-3}$) established by the World Health Organization [40]: 21% (3/14) in the summer, 86% (12/14) in the autumn, and 86% (12/14) in the winter. Similarly, the 24-h $PM_{2.5}$ National Ambient Air Quality Standard (NAAQS) of 35 $\mu g\ m^{-3}$ [41] was exceeded by 12% (5/14) in the autumn and 7% (3/14) in the winter. In contrast, the 24-h standard (45 $\mu g\ m^{-3}$) established by the NOM-025-SSA1-2014 [42] was surpassed by only 5% (2/14) during the winter.

Table 1. Descriptive statistics of 24-h average $PM_{2.5}$ concentrations in sites M1, M2, and M3 during different seasons.

Season	Parameter ($PM_{2.5}$ μg m^{-3})	Site M1 (Ref US)	M2 (Ref MX)	M3 (SYPOE)
Summer 2018	Mean	10.8	14.7	13.6
	Median	9.8	14.4	12.6
	Q1	8.0	10.2	11.6
	Q3	12.6	17.3	14.2
	Range	5.4–17.7	6.0–24.0	8.9–27.2
	N	14	12	14
Autumn 2018	Mean	11.8	21.5	28.7
	Median	10.7	18.5[1]	27.2 [1]
	Q1	8.6	17.6	22.9
	Q3	13.4	24.5	36.6
	Range	4.7–23.1	7.5–45.8	13.5–41.5
	N	14	14	14
Winter 2018	Mean	13.2	21.9	28.2
	Median	10.3	21.0[1]	23.4[1]
	Q1	8.1	18.7	17.7
	Q3	20.0	24.6	30.1
	Range	4.9–23.8	8.3–41.9	14.4–77.5
	N	14	13	14
Entire campaign	Mean	11.9	19.5	23.5
	Median	10.3 [2]	18.2[2]	19.5 [2]
	Q1	8.2	13.0	14.1
	Q3	15.0	24.2	28.9
	Range	4.7–23.8	6.0–45.8	8.9–77.5
	N	42	39	42

[1] Data from sites M2 and M3 are significantly higher than site M1 ($p < 0.05$). [2] Kruskal–Wallis. M3 = M2 > M1.

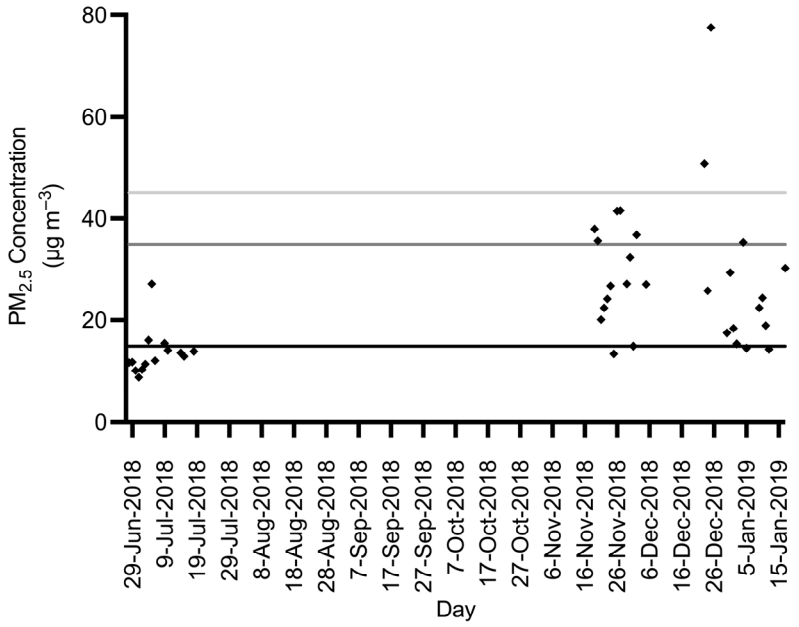

Figure 2. Time series of 24-h $PM_{2.5}$ at site M3 during the summer, autumn, and winter of 2018 compared to the guidelines: dark blackline (WHO, 15 μg m^{-3}); dashed line (NAAQS, 35 μg m^{-3}); light gray (NOM−025-SSA1−2014, 45 μg m^{-3}).

The maximum value of $PM_{2.5}$ in the summer of 2018 was 27.2 μg m^{-3}, registered on 5 July, following US Independence Day celebrations. In their corresponding studies,

both Seidel and Birnbaum and Mendez et al. reported increases of $PM_{2.5}$ associated with Independence Day celebrations in several cities of the US on the night of 4 July and the morning of 5 July [43,44]. In another incident at the border, maxima of 41.4 μg m^{-3} and 41.5 μg m^{-3} were each measured on 26 and 27 November 2018, which matched the arrival of a migrant caravan coming from Honduras. During this event, there were increased emissions from vehicles and helicopters patrolling the area. Comparably, the maximum $PM_{2.5}$ concentration measured in winter was 77.5 μg m^{-3}, registered on 25 December 2018. This value is likely associated with Christmas celebrations, which usually include fireworks. Singh et al. reported how the use of fireworks elevates ambient $PM_{2.5}$ [45].

Jansen et al. indicated that $PM_{2.5}$ concentrations > 20 μg m^{-3} exacerbate the symptoms of subjects with asthma and increase the risk correlated with lung cancer, mortality, and cardiovascular disease by 4, 6, and 8%, respectively [46]. Other findings suggest that asthmatic patients experience greater oxidation of plasmatic fluids due to $PM_{2.5}$ exposure and increased ROS generated by neutrophils [47]. In this study, 59% of the samples (25/42) in the entire sampling campaign were above 20 μg m^{-3}; therefore, the concentrations logged herein could exacerbate the health problems of vulnerable populations.

3.3. Effect of Meteorological Conditions on $PM_{2.5}$ Concentrations

Over the period of this research, there was a predominantly southwest to northeast wind direction in summer (Figure S1); as for autumn, the predominant direction was from the west [48], while the direction in winter was from the northeast.

A negative correlation ($p < 0.05$) was determined between temperature and $PM_{2.5}$ concentrations for autumn ($\rho = -0.61$) and summer ($\rho = -0.69$), as shown in Table S5; this was not the case for winter, as no connection was detected. Moreover, the mean wind speeds in summer were 11% to 37% higher than those of autumn and winter, respectively, further favoring the dispersion of pollutants.

In the autumn of 2018, there was a negative correlation ($p < 0.05$) between the daily concentration of $PM_{2.5}$ and wind speed ($\rho = -0.55$). In a study conducted in 2010, Quintana et al. reported median $PM_{2.5}$ concentrations near the SYPOE of 30.2 (February–March), 19.2 (April−June), and 4.2 μg m^{-3} (November) [4]. That study deduced that pollution concentrations were higher during lower wind speeds or when the wind was blowing from the SYPOE toward their sampling site.

3.4. Temporal Variability of Black Carbon

Table 2 displays descriptive statistics per season for BC. The results revealed that the autumn and winter of 2018 had higher concentrations than the spring and summer of 2018. Similarly, BC concentrations in the autumn and winter of 2017 were 1.2 and 2 times those of 2018, respectively; the lower precipitation periods registered in autumn-winter 2017 (0.04/0.02 mm) may explain these differences when compared to 2018 (57.3/43.8 mm).

BC concentrations on weekdays and weekends were compared too, and the results are shown in Table 2. The highest BC weekday concentrations were significantly higher ($p < 0.05$) than those of weekends during autumn to winter in 2017. These results highlight the influence of activities related to work and school.

Figure S2 presents the 1-h average BC concentrations as a time series during the entire campaign. In autumn of 2017 (namely on 24 November), the maximum value of 77.7 μg m^{-3} coincided with "Black Friday", a popular sale day in the US, leading to a rise in traffic movements from Mexico to San Ysidro. Other common sources of BC are clandestine open fires on the Mexican side, which could raise local concentrations during autumn and winter seasons. The maximum BC concentrations in winter were 148.9 μg m^{-3} (24 December 2018) and 54.3 μg m^{-3} (1 January 2019). Both dates coincide with important holidays (i.e., Christmas and the New Year) and are likely the combined results of fireworks, bonfires, and clandestine open fires. In a study performed considering both the US and Mexico, Takahama et al. detected peaks of high concentrations of BC, thus suggesting clandestine burning activities [49].

Table 2. Descriptive statistics of 1-h average BC concentrations in the entire campaign, during weekdays and weekends for each studied season.

Period	BC ($\mu g\ m^{-3}$)	Autumn 2017	Winter 2017	Spring 2018	Summer 2018	Autumn 2018	Winter 2018
Entire campaign	Average	3.7	5.7	0.6	0.7	5.6	5.3
	Median	2.1 *	3.8 *	0.4	0.4	1.3 *	1.9 *
	Q1	1.1	1.8	0.2	0.3	0.1	0.8
	Q3	4.1	7.4	0.6	0.7	3.9	4.4
	Maximum	77.7	42.0	6.2	7.5	82.4	148.9
	N	409	362	336	365	337	361
Weekdays	Average	2.2	6.2	0.4	0.7	5.9	6.1
	Median	2.3 **	3.9 **	0.3 **	0.4 **	1.5	1.8
	Q1	1.1	2.0	0.2	0.3	0.4	0.8
	Q3	4.3	7.7	0.5	0.8	4.8	4.4
	Maximum	77.7	42	4.0	7.5	82.4	148.9
	N	313	250	240	271	217	281
Weekends	Average	1.8	4.7	0.5	0.5	6.2	2.8
	Median	1.6	3.5	0.6	0.4	1.4	1.9
	Q1	1.1	1.3	0.3	0.3	0.3	0.8
	Q3	3.1	6.2	0.8	0.6	4.2	3.7
	Maximum	15.5	39.2	6.2	1.6	67.3	16.3
	N	159	112	96	95	96	80

* Significantly higher than the summer and spring of 2018, $p < 0.05$. ** Significantly higher than weekends, $p < 0.05$.

3.5. Effect of Meteorological Conditions on BC Concentrations

Spearman correlations between 1-h average BC concentrations and meteorological conditions (temperature, RH, barometric pressure, precipitation, and wind speed) were calculated and are included in Table S6.

There was a moderate negative correlation (p <0.05) established between BC concentrations and the temperature in winter in 2017 ($\rho = -0.65$) and 2018 ($\rho = -0.51$). Other studies have shown a negative relationship between temperature and BC concentrations.

A moderate negative correlation ($p < 0.05$) was also determined for wind speed and BC concentration during the autumn of 2017 ($\rho = -0.51$), winter of 2017 ($\rho = -0.54$), autumn of 2018 ($\rho = -0.56$) and winter of 2018 ($\rho = -0.59$). Table 3 exhibits significantly higher BC concentrations during low wind speed (<5 m s^{-1}) periods compared to other wind speeds (>5 m s^{-1}) for autumn in 2017, summer in 2018, autumn in 2018, and winter in 2018. These lower wind speeds decrease dispersion, resulting in greater BC concentrations. Quintana et al. previously reported that 1-h average BC concentrations were higher during periods with lower wind speeds compared to higher ones (>0.5 m s^{-1}) [4].

Furthermore, the impact of wind direction on BC concentrations was investigated. The rise in pollution (Figure S3) highlights pollutant transport from the southwest (Tijuana) to the northeast (San Ysidro) in spring and summer. This behavior has been reported before by Shores et al. and Bei et al. [50,51]. The pollutant transport in autumn (2017 and 2018) and winter (2017 and 2018) occurred with a northeast to southwest direction. In the same way, contributions from the west indicated impacts from both the urban area and the SYPOE. The influence of the northeast to southwest direction denoted the transport of pollutants from the SYPOE toward Tijuana. Therefore, any strategy to reduce pollutants at the border crossing must consider the associated transport of pollutants.

Table 3. Descriptive statistics of 1-h average BC concentrations during low and other wind speeds in the different seasons studied.

BC Conc. (μg m^{-3})		Autumn 2017	Winter 2017	Spring 2018	Summer 2018	Autumn 2018	Winter 2018
low wind speed	Average	5.0	5.3	0.3	1.1	8.6	5.8
	Median	3.2 *	4.0	0.4	0.8 *	3.2 *	2.6 *
	Q1	1.8	2.8	0.3	0.5	1.8	1.4
	Q3	6.0	6.4	0.9	1.5	12.6	5.0
	Maximum	77.7	27.4	4.0	3.6	45.6	94.8
	N	141	81	33	47	38	60
other wind speed	Average	3.0	5.8	0.6	0.6	5.5	5.2
	Median	1.5	3.6	0.4	0.4	1.4	1.7
	Q1	0.9	1.6	0.2	0.3	0.3	0.7
	Q3	3.2	7.8	0.6	0.6	4.0	4.0
	Maximum	21.1	42.0	6.2	7.5	82.4	148.9
	N	268	281	303	318	299	301

* Significantly higher than other wind speeds (>0.5 m s^{-1}), $p < 0.05$.

3.6. Diurnal Behavior

The diurnal behavior of BC concentration is presented in Figure 3. The results point out increased BC concentrations in the morning (4:00 a.m. to 9:00 a.m.), which reflects the start of anthropogenic activities, like the morning commute. An additional rise was observed around 6:00 p.m., coinciding with the evening commute; similar daily diurnal patterns of high concentrations from 7:00 a.m. to 9:00 a.m. have been registered for different urban areas [52–56]. In the present study, these activities began earlier in the morning, starting around 4:00 a.m., because people working or studying in the US and living in Tijuana must also cross the border, adding time to their daily commute [57].

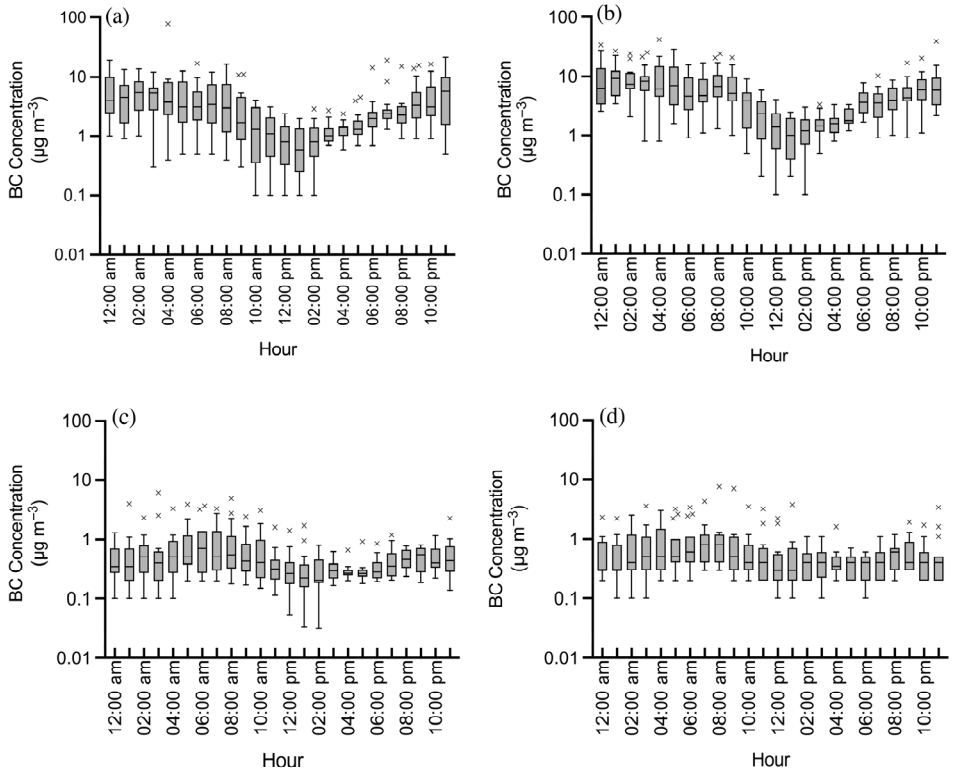

Figure 3. *Cont.*

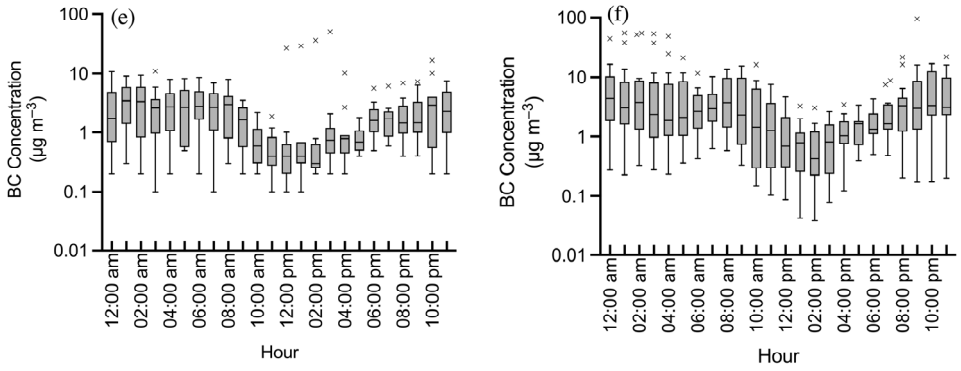

Figure 3. Box and whisker plot of the diurnal variation of BC concentration at the SYPOE: (**a**) autumn of 2017, (**b**) winter of 2017, (**c**) spring of 2018, (**d**) summer of 2018, (**e**) autumn of 2018, (**f**) winter of 2018. The × indicates outliers.

3.7. BC and $PM_{2.5}$ Correlation and Ratio

BC and $PM_{2.5}$ were found to be moderately positively correlated ($p < 0.05$) for summer ($\rho = 0.69$), autumn ($\rho = 0.52$), and winter ($\rho = 0.59$); this indicates that they likely come from similar sources [58]. This result agrees with reports from other urban sites [53,59]. In addition, the ratio of BC/$PM_{2.5}$ has been shown to vary significantly (0.03–0.77) among mobile sources [58] and has been used to identify specific sources. Daily BC/$PM_{2.5}$ ratios were calculated and are presented in Table S7. The mean BC/$PM_{2.5}$ for winter was 0.1, which is associated with non-road gasoline sources; the highest BC/$PM_{2.5}$ ratio for winter was 0.7, which is related to non-road diesel sources. Ratio variations may be due to speed, weight load, and driving conditions. Gaitan et al. registered BC/$PM_{2.5}$ ratios ranging from 0.02–0.10, connected with gasoline vehicle emissions in Monterrey, Mexico [60]. Meanwhile, Liu et al. logged BC/$PM_{2.5}$ ratios ranging from 0.02 to 0.27 in Beijing, China [61], linked to traffic emissions. In this study, the emissions encompass those from diesel sources, unlike the aforementioned studies.

3.8. Oxidative Potential

The oxidative potential associated with $PM_{2.5}$ considered during the entire sampling campaign is represented in Figure 4. The median values of OP_{DTTm} (and OP_{DTTv}) in summer, autumn, and winter were 12.7 (0.2), 11.7 (0.3), and 18.5 (0.6) pmol min^{-1} µg^{-1} (nmol min^{-1} m^{-3}), respectively. Gao et al. and Molina et al. also noted higher OP_{DTTm} and OP_{DTTv} in the colder seasons [34,62]. Shirmohammadi et al. reported OP_{DTTm} increases of 40–90% (OP_{DTTv} of 20–40%) in colder months when compared to the warmer months in samples collected in Los Angeles, USA [63].

Abrams et al. proposed OP_{DTTv} as an indicator of air pollution toxicity, establishing a relation between OP_{DTTv} and cardiorespiratory emergency department visits [21]. Delfino et al. found boosts of 8.7–9.9% in exhaled nitric oxide (a biomarker of airway inflammation) related to an interquartile range of OP_{DTTv} of 0.43 nmol min^{-1} m^{-3} in children from 9 to 18 years [64]. In this research, OP_{DTT} values > 0.43 nmol min^{-1} m^{-3} were found on 77% of the winter sampling days, suggesting that the probability of having respiratory disease complications is higher during this season.

On the other hand, the OP_{DTT} for summer and autumn were not significantly different ($p > 0.05$). OP_{DTT} in autumn was positively correlated to the waiting time of vehicles crossing the SYPOE ($\rho = 0.673$, $p < 0.05$), considering site M3 was located 200 m away. Cho et al. reported higher OP_{DTT} in areas near traffic [65]; therefore, the influence of vehicles waiting and the correlation with population exposure should be considered.

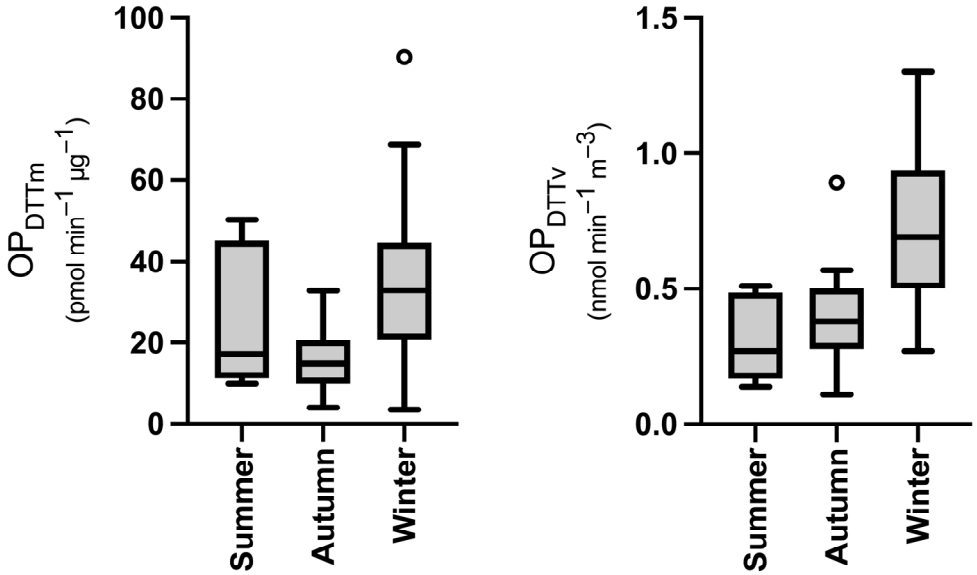

Figure 4. Oxidative potential (OP_{DTT}) associated with $PM_{2.5}$ during the different seasons of the year at the sampling site. The circle indicates outliers.

The OP_{DTT} values determined in this study are comparable to those in Los Angeles, US (15–54 pmol min^{-1} μg^{-1}), Fresno, US (27–61 pmol min^{-1} μg^{-1}), and Chillan, Chile (4–32 pmol min^{-1} μg^{-1}) [33,34,66].

3.9. Exposure and Inhalation Dose of BC

Table 4 exhibits the median 24-h average BC concentrations for all seasons included in this research. The highest daily average and median values were registered in 2017.

Table 4. Descriptive statistics of 24-h average BC concentrations during the different studied seasons.

Parameter ($\mu g\ m^{-3}$)	Autumn 2017	Winter 2017	Spring 2018	Summer 2018	Autumn 2018	Winter 2018
Average	3.7	5.7	0.9	0.7	7.1	5.4
Median	3.0	5.1	0.5	0.5	4.2	3.9
Q1	1.9	3.8	0.3	0.4	2.0	1.5
Q3	4.7	6.6	0.9	0.8	10.5	5.1
Maximum	9.4	13.2	0.5	2.3	21.2	18.3
N	17	15	14	15	11	15

Madrigano et al. pointed out that human exposure to an ambient BC concentration of 1.77 $\mu g\ m^{-3}$ in a 24-h period is linked with inflammation and decreased endothelial function [67]. Jansen et al. reported increments of 11.2% in fractional exhaled nitric oxide for asthmatic children for BC concentrations of 3 $\mu g\ m^{-3}$ in a 24-h period [46]. Increases in fractional exhaled nitric oxide for asthmatic children also worsened the respiratory effects. The BC concentrations in this study, autumn, and winter levels were >3 $\mu g\ m^{-3}$ in a 24-h period, raising similar concerns.

The estimated (95 percentile) pedestrian waiting time, average BC concentration, and inhalation dose of BC for each season are displayed in Table 5. The highest doses were assessed for autumn in 2018 and winter in 2017; notably, a pedestrian waiting time of 50 min in winter in 2017 led to a BC inhalation dose eight times higher than in spring in 2018.

Table 5. Inhalation dose (μg) of BC as a function of pedestrian and workers, per season.

Season	Pedestrian Waiting Time min (95 Percentile)	Average BC Concentration (μg m^{-3})	Pedestrian Inhalation Dose [1] (μg)	Workers Inhalation Dose [2] (μg)
Autumn, 2017	58	5.0	2.5	12.0
Winter, 2017	50	8.2	3.5	19.0
Spring, 2018	50	0.9	0.4	3.9
Summer, 2018	65	1.0	0.6	3.5
Autumn, 2018	60	11.6	5.9	13.0
Winter, 2018	60	5.0	2.6	10.6

[1] Inhalation dose was estimated for a pedestrian waiting time in minutes on a travel day. [2] Inhalation dose was estimated for a day of work (average time of 10 h).

Liu et al. documented an inhalation dose of 5.7 μg for walking in Macau, China (60 min) during traffic hours (7:30 a.m.–9:00 a.m.) [54], a dose comparable to the value of 5.9 μg for autumn in 2018 according to this research. Velasco et al. estimated an inhalation dose of BC of 6.0 μg for people walking (60 min) in Mexico City during winter [68]. This study estimated 60-min doses of 4.2 and 2.6 μg for the winters of 2017 and 2018, respectively, which are congruent to those reported in other urban environments.

Table 5 also shows the 24-h inhalation dose for workers at the border, with an average 10-h shift per day considering 6 d per week. For the workers, a daily dose was estimated based on their individual working schedule, resulting in ranges from 3.5 to 19 μg (Figure S4). These 24-h values are two to nine times higher than the estimated daily dose for pedestrians during their crossing. Furthermore, a worker at this crossing received an annual inhalation dose of 28.2 mg of BC in 2018. A year-long exposure to BC is associated with a declining annual growth of working memory [69].

Figure 5 depicts the diurnal distribution of BC inhalation dose for winter in 2017, which registered the highest doses in this study. To reduce the daily inhalation dose, workers should avoid the periods between 7:00 to 9:00 a.m. and 7:00 to 9:00 p.m. Another option would be for workers in these periods to have rotating schedules or to work fewer days at times with lower inhalation doses.

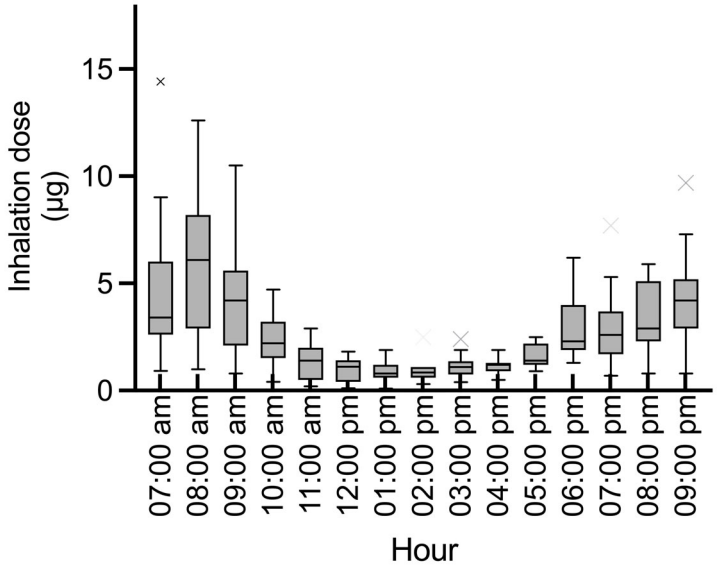

Figure 5. Box and whisker plot of diurnal distribution of inhalation dose of BC for workers at the SYPOE in the winter of 2017.

4. Conclusions

There is a lack of government-sponsored air quality monitors near the SYPOE on either side of the border. This study provides the first measurements of $PM_{2.5}$ and BC concentrations on the Mexican side of the SYPOE. This is also the first reported oxidative potential (per OP_{DTT}) of $PM_{2.5}$ measured along the US–Mexico border. These measurements

could be useful at all border crossings to identify periods with poor air quality conditions that may lead to adverse health effects for border crossers, workers, and nearby residents.

The highest inhalation doses of BC for pedestrians in this study occurred in the early morning when the concentrations were highest. Decreasing waiting times for pedestrians on days with high air pollution would reduce their inhalation doses and implied health risks. On the other hand, limiting doses for workers may require modifying their schedule to lessen their exposure. These recommendations would partially address environmental justice in the border area. Waiting times might be augmented by stricter immigration policies or events such as COVID-19, as previously indicated by Quintana et al. with the 9/11 incident [4]. This could lead to increased exposure for both pedestrians and workers.

This information could be transferred to other traffic areas where there are people stationed at exposed traffic lights, school drop-off and pick-up points, or peddlers close to busy streets for long periods.

The conclusions drawn from this study are limited by the number of samples collected in each season and the use of a single indirect health metric (OP_{DTT}). Increasing the number of samples per season and additional health metrics would allow higher levels of confidence in these results.

This study only considers adults, while inhalation doses in children would be higher. Similarly, the inhalation doses for pedestrians and workers documented herein only correspond to the border; they do not account for other microenvironments where people spend the rest of their day. More comprehensive studies could include the chemical composition of $PM_{2.5}$ and health information about the populations that cross, work, and live near the SYPOE. This research provides an initial assessment of an understudied issue: the exposure of workers at the border. Studies focused on this population would lead to a better understanding of the challenges faced by this population, including those related to environmental justice.

Supplementary Materials: The following supporting information can be downloaded at: https://www.mdpi.com/article/10.3390/environments11060128/s1, Table S1: Description of the sampling campaign; Table S2: Meteorological condition during the study; Table S3: Descriptive statistics of waiting time for pedestrians and vehicles during the crossing in SYPOE; Table S4: Descriptive statistics of answers to the survey conducted to border workers; Table S5: Spearman correlations between 24-h averaged $PM_{2.5}$ concentrations and meteorological conditions during the study; Figure S1: Wind roses during: (a) autumn 2017, (b) winter 2017, (c) spring 2018, (d) summer 2018, (e) autumn 2018, and (f) winter 2018; Figure S2: Time series of 1-h average log BC concentration in the SYPOE during (a) autumn 2017, (b) winter 2017, (c) spring 2018, (d) summer 2018, (e) autumn 2018, and (f) winter 2018; Table S6: Spearman correlations between 1-h averaged BC concentrations and meteorological condition during the study; Figure S3: Pollution roses for BC concentration during: (a) autumn 2017, (b) winter 2017, (c) spring 2018, (d) summer 2018, (e) autumn 2018, and (f) winter 2018; Table S7: $BC/PM_{2.5}$ ratios; Figure S4: Diurnal variation of inhalation dose of BC at the SYPOE: (a) autumn 2017, (b) winter 2017, (c) spring 2018, (d) summer 2018, (e) autumn 2018, (f) winter 2018.

Author Contributions: R.Z.: Investigation and writing—original draft. P.J.E.Q.: Resources, writing—reviewing and editing. Y.T.-M.: Writing—reviewing and editing, visualization, and formal analysis. F.T.W.: Formal analysis. L.D.M.: Writing—reviewing and editing. J.E.C.: Investigation, supervision, and writing—reviewing and editing. All authors have read and agreed to the published version of the manuscript.

Funding: This work was financed by the Consejo de Desarrollo Económico de Tijuana through the Fideicomiso Empresarial del Estado de Baja California (FIDEM) 2017 (PT-1703e-057) and was partially supported by a scholarship to R. Zurita (number of scholarships 480889) from the Consejo Nacional de Ciencia y Tecnología (CONACYT).

Data Availability Statement: The datasets generated during and/or analyzed during the current study are available in the datasets related to this article and can be found at http://dx.doi.org/10.17632/3zb8vkpnyx.1 (accessed on 26 November 2020), an open-source online data repository hosted at Mendeley Data [70].

Acknowledgments: The authors gratefully acknowledge the support of the association of merchants located on the border of the Mexican side for providing us with the facilities to carry out the sampling.

Conflicts of Interest: The authors declare no conflicts of interest. The funders had no role in the design of the study; in the collection, analyses, or interpretation of data; in the writing of the manuscript; or in the decision to publish the results.

References

1. Censo de Población y Vivienda- Instituto Nacional de Estadística y Geografía (INEGI). Available online: https://www.inegi.org.mx/programas/ccpv/2020/ (accessed on 21 July 2021).
2. U.S. Census Bureau-American Community Survey 1-Year Estimates. Available online: https://www.census.gov/programs-surveys/acs. (accessed on 23 July 2021).
3. Secretaría de Medio Ambiente y Recursos Naturales (SEMARNAT); US Environmental Protection Agency (US EPA). *United States-Mexico Environmental Program: Border 2020*; SEMARNAT and US EPA: Tijuana, Mexico, 2012. [CrossRef]
4. Quintana, P.J.E.; Dumbauld, J.J.; Garnica, L.; Chowdhury, M.Z.; Velascosoltero, J.; Mota-Raigoza, A.; Flores, D.; Rodríguez, E.; Panagon, N.; Gamble, J.; et al. Traffic-Related Air Pollution in the Community of San Ysidro, CA, in Relation to Northbound Vehicle Wait Times at the US-Mexico Border Port of Entry. *Atmos. Environ.* **2014**, *88*, 353–361. [CrossRef]
5. California Air Resources Board (CARB). Available online: https://ww2.arb.ca.gov/es/news/carb-incrementa-el-numero-de-comunidades-en-desventaja-nivel-estatal-en-el-programa-de (accessed on 11 April 2022).
6. US Customs and Border Protection (CBP). Border Wait Times. 2019. Available online: http://apps.cbp.gov/bwt/ (accessed on 1 January 2019).
7. San Diego Association of Governments (SANDAG). Border Wait Time Technologies and Information Systems White Paper. San Diego, CA. 2020. Available online: https://www.sandag.org/uploads/publicationid/publicationid_4469_23227.pdf (accessed on 11 May 2022).
8. Galaviz, V.E.; Yost, M.G.; Simpson, C.D.; Camp, J.E.; Paulsen, M.H.; Elder, J.P.; Hoffman, L.; Flores, D.; Quintana, P.J.E. Traffic Pollutant Exposures Experienced by Pedestrians Waiting to Enter the U.S. at a Major U.S.-Mexico Border Crossing. *Atmos. Environ.* **2014**, *88*, 362–369. [CrossRef]
9. Quintana, P.J.E.; Ganster, P.; Stigler Granados, P.E.; Muñoz-Meléndez, G.; Quintero-Núñez, M.; Rodríguez-Ventura, J.G. Risky Borders: Traffic Pollution and Health Effects at US–Mexican Ports of Entry. *J. Borderl. Stud.* **2015**, *30*, 287–307. [CrossRef]
10. Mukherjee, A.; Mccarthy, M.C.; Brown, S.G.; Huang, S.; Landsberg, K.; Eisinger, D.S. Influence of Roadway Emissions on Near-Road PM2.5: Monitoring Data Analysis and Implications. *Transp. Res. Part D Transp. Environ.* **2020**, *86*, 102442. [CrossRef]
11. Karner, A.A.; Eisinger, D.S.; Niemeier, D.A. Near-Roadway Air Quality: Synthesizing the Findings from Real-World Data. *Environ. Sci. Technol.* **2010**, *44*, 5334–5344. [CrossRef]
12. Lee, Y.G.; Lee, P.H.; Choi, S.M.; An, M.H.; Jang, A.S. Effects of Air Pollutants on Airway Diseases. *Int. J. Environ. Res. Public Health* **2021**, *18*, 9905. [CrossRef]
13. Miller, M.R.; Newby, D.E. Air Pollution and Cardiovascular Disease. *Cardiovasc. Res.* **2020**, *116*, 279–294. [CrossRef] [PubMed]
14. Marsal, A.; Sauvain, J.J.; Thomas, A.; Lyon-Caen, S.; Borlaza, L.J.S.; Philippat, C.; Jaffrezo, J.L.; Boudier, A.; Darfeuil, S.; Elazzouzi, R.; et al. Effects of Personal Exposure to the Oxidative Potential of PM2.5 on Oxidative Stress Biomarkers in Pregnant Women. *Sci. Total Environ.* **2024**, *911*, 168475. [CrossRef] [PubMed]
15. Vega, E.; Ruiz, H.; Escalona, S.; Cervantes, A.; Lopez-Veneroni, D.; Gonzalez-Avalos, E.; Sanchez-Reyna, G. Chemical Composition of Fine Particles in Mexico City during 2003–2004. *Atmos. Pollut. Res.* **2011**, *2*, 477–483. [CrossRef]
16. Xie, J.; Jin, L.; Cui, J.; Luo, X.; Li, J.; Zhang, G.; Li, X. Health Risk-Oriented Source Apportionment of PM2.5-Associated Trace Metals. *Environ. Pollut.* **2020**, *262*, 114655. [CrossRef]
17. Moufarrej, L.; Verdin, A.; Cazier, F.; Ledoux, F.; Courcot, D. Oxidative Stress Response in Pulmonary Cells Exposed to Different Fractions of PM2.5-0.3 from Urban, Traffic and Industrial Sites. *Environ. Res.* **2023**, *216*, 114572. [CrossRef] [PubMed]
18. Bates, J.T.; Fang, T.; Verma, V.; Zeng, L.; Weber, R.J.; Tolbert, P.E.; Abrams, J.Y.; Sarnat, S.E.; Klein, M.; Mulholland, J.A.; et al. Review of Acellular Assays of Ambient Particulate Matter Oxidative Potential: Methods and Relationships with Composition, Sources, and Health Effects. *Environ. Sci. Technol.* **2019**, *53*, 4003–4019. [CrossRef]
19. Zhang, X.; Staimer, N.; Tjoa, T.; Gillen, D.L.; Schauer, J.J.; Shafer, M.M.; Hasheminassab, S.; Pakbin, P.; Longhurst, J.; Sioutas, C.; et al. Associations between Microvascular Function and Short-Term Exposure to Traffic-Related Air Pollution and Particulate Matter Oxidative Potential. *Environ. Health* **2016**, *15*, 81. [CrossRef] [PubMed]
20. Bates, J.T.; Weber, R.J.; Abrams, J.; Verma, V.; Fang, T.; Klein, M.; Strickland, M.J.; Sarnat, S.E.; Chang, H.H.; Mulholland, J.A.; et al. Reactive Oxygen Species Generation Linked to Sources of Atmospheric Particulate Matter and Cardiorespiratory Effects. *Environ. Sci. Technol.* **2015**, *49*, 13605–13612. [CrossRef]
21. Abrams, J.Y.; Weber, R.J.; Klein, M.; Samat, S.E.; Chang, H.H.; Strickland, M.J.; Verma, V.; Fang, T.; Bates, J.T.; Mulholland, J.A.; et al. Associations between Ambient Fine Particulate Oxidative Potential and Cardiorespiratory Emergency Department Visits. *Environ. Health Perspect.* **2017**, *125*, 1–9. [CrossRef]

22. Janssen, N.A.H.; Hoek, G.; Simic-Lawson, M.; Fischer, P.; van Bree, L.; ten Brink, H.; Keuken, M.; Atkinson, R.W.; Ross Anderson, H.; Brunekreef, B.; et al. Black Carbon as an Additional Indicator of the Adverse Health Effects of Airborne Particles Compared with PM10 and PM2.5. *Environ. Health Perspect.* **2011**, *119*, 1691–1699. [CrossRef]
23. Sarnat, S.E.; Raysoni, A.U.; Li, W.W.; Holguin, F.; Johnson, B.A.; Luevano, S.F.; Garcia, J.H.; Sarnat, J.A. Air Pollution and Acute Respiratory Response in a Panel of Asthmatic Children along the U.S.-Mexico Border. *Environ. Health Perspect.* **2012**, *120*, 437–444.
24. Quintana, P.J.E.; Stigler, P.; Muñoz-Meléndez, G.; Quintero-Núñez, M.; Rodríguez-Ventura, J.G. White paper: Health impacts of crossings at US-Mexico land ports of entry: Gaps, needs and recommendations for action. In *Report from the Health Impacts of Border Crossings*; 2012 Conference May 3 and 4; San Diego State University: San Ysidro, CA, USA, 2012. Available online: https://kpbs.media.clients.ellingtoncms.com/news/documents/2013/05/15/Health_Impacts_of_Border_Crossings_White_Paper_FINAL.pdf (accessed on 3 June 2020).
25. Carrillo, G.; Uribe, F.; Lucio, R.; Ramirez Lopez, A.; Korc, M. The United States-Mexico Border Environmental Public Health: The Challenges of Working with Two Systems. *Pan Am. J. Public Health* **2017**, *41*, 98. [PubMed]
26. NOAA National Estuarine Research Reserve System (NERRS). Available online: http://cdmo.baruch.sc.edu/data/available-data/ (accessed on 2 October 2020).
27. Secretaria de Salud. Mexicana PROY-NMX-AA-177-SCFI-2015, Equivalent Reference Methods for the Measurement of PM10 and PM2.5 Suspended Particles in the Air. Diario Oficial de la Federacion. 2015. Available online: https://caisatech.net/uploads/XXI_2_MXD_E39_PROY-NMX-AA-177-%20SCFI-2015_R0_24FEB2016.pdf (accessed on 5 February 2021).
28. Tisch Environmental Inc. Operations Manual, Particulate Matter 10 Microns and Less High-Volume Air Sampler. 2010. Available online: https://tisch-env.com/high-volume-air-sampler/pm2.5 (accessed on 15 October 2020).
29. US Environmental Protection Agency (US EPA). *Standard Operating Procedure for the Mass Analysis and Subsequent Extraction of Sampled PM10 and Tsp from Exposed Quartz and Glass Microfiber Filters*; US EPA: Washington, DC, USA, 2002.
30. Hagler, G.S.W.; Yelverton, T.L.B.; Vedantham, R.; Hansen, A.D.A.; Turner, J.R. Post-processing Method to Reduce Noise while Preserving High Time Resolution in Aethalometer Real-time Black Carbon Data. *Aerosol Air Qual. Res.* **2011**, *11*, 539–546. [CrossRef]
31. Virkkula, A.; Mäkelä, T.; Hillamo, R.; Yli-Tuomi, T.; Hirsikko, A.; Hämeri, K.; Koponen, I.K. A Simple Procedure for Correcting Loading Effects of Aethalometer Data. *J. Air Waste Manag. Assoc.* **2007**, *57*, 1214–1222. [CrossRef]
32. Fang, T.; Verma, V.; Guo, H.; King, L.E.; Edgerton, E.S.; Weber, R.J. A Semi-Automated System for Quantifying the Oxidative Potential of Ambient Particles in Aqueous Extracts Using the Dithiothreitol (DTT) Assay: Results from the Southeastern Center for Air Pollution and Epidemiology (SCAPE). *Atmos. Meas. Tech.* **2015**, *8*, 471–482. [CrossRef]
33. Charrier, J.G.; Anastasio, C. On Dithiothreitol (DTT) as a Measure of Oxidative Potential for Ambient Particles: Evidence for the Importance of Soluble Transition Metals. *Atmos. Chem. Phys.* **2012**, *12*, 11317–11350. [CrossRef] [PubMed]
34. Molina, C.; Manzano, C.A.; Toro, R.; Leiva, G.M.A. The Oxidative Potential of Airborne Particulate Matter in Two Urban Areas of Chile: More than Meets the Eye. *Environ. Int.* **2023**, *173*, 107866. [CrossRef]
35. Ott, W.R. Concepts of Human Exposure to Air Pollution. *Environ. Int.* **1982**, *7*, 179–196. [CrossRef]
36. US Environmental Protection Agency (US EPA). *Exposure Factors Handbook 2011 Edition (Final Report)*; EPA/600/R-09/052F; U.S. Environmental Protection Agency: Washington, DC, USA, 2011. Available online: https://cfpub.epa.gov/si/si_public_record_report.cfm?Lab=NCEA&dirEntryId=236252 (accessed on 5 January 2020).
37. Instituto Nacional de Ecologia y Cambio Climatico (INECC), Secretaria de Medio Ambiente y Recursos Naturales (SEMARNAT). Study of Emissions and Vehicular Activity in Baja California, Mexico. Final Report. 2011. Available online: https://www.gob.mx/cms/uploads/attachment/file/112408/2011_CGCSA_RSD_Baja_California.pdf (accessed on 25 March 2019).
38. Zavala, M.; Barrera, M.; Morante, H.; Molina, J.; Zavala, M.; Barrera, H.; Morante, J.; Molina, L.T. Analysis of Model-Based $PM_{2.5}$ Emission Factors for on-Road Mobile Sources in Mexico. *Atmósfera* **2013**, *26*, 109–124. [CrossRef]
39. Smith, L.A.; Mukerjee, S.; Monroy, G.J.; Keene, F.E. Preliminary Assessments of Spatial Influences in the Ambos Nogales Region of the US–Mexican Border. *Sci. Total Environ.* **2001**, *276*, 83–92. [CrossRef] [PubMed]
40. World Health Organization (WHO). Ambient (Outdoor) Air Pollution. Available online: https://www.who.int/news-room/fact-sheets/detail/ambient-(outdoor)-air-quality-and-health (accessed on 28 October 2021).
41. US Environmental Protection Agency (US EPA). NAAQS Table. Available online: https://www.epa.gov/criteria-air-pollutants/naaqs-table (accessed on 20 December 2019).
42. Secretaria de Salud. NORMA Oficial Mexicana NOM-025-SSA1-2014. Available online: http://siga.jalisco.gob.mx/aire/normas/NOM-025-SSA1-2014.pdf (accessed on 5 January 2020).
43. Seidel, D.J.; Birnbaum, A.N. Effects of Independence Day Fireworks on Atmospheric Concentrations of fine Particulate Matter in the United States. *Atmos. Environ.* **2015**, *115*, 192–198. [CrossRef]
44. Mendez, E.; Temby, O.; Wladyka, D.; Sepielak, K.; Raysoni, A.U. Fine Particulate Matter Concentrations during Independence Day Fireworks Display in the Lower Rio Grande Valley Region, South Texas, USA. *Sci. World J.* **2022**, *2022*, 8413574. [CrossRef]
45. Singh, A.; Pant, P.; Pope, F.D. Air Quality during and after Festivals: Aerosol Concentrations, composition and health effects. *Atmos. Res.* **2019**, *227*, 220–232. [CrossRef]
46. Jansen, K.L.; Larson, T.V.; Koenig, J.Q.; Mar, T.F.; Fields, C.; Stewart, J.; Lippmann, M. Associations between Health Effects and Particulate Matter and Black Carbon in Subjects with Respiratory Disease. *Environ. Health Perspect.* **2005**, *113*, 1741–1746. [CrossRef]

47. Sierra-Vargas, M.P.; Guzman-Grenfell, A.M.; Blanco-Jimenez, S.; Sepulveda-Sanchez, J.D.; Bernabe-Cabanillas, R.M.; Cardenas-Gonzalez, B.; Ceballos, G.; Hicks, J.J. Airborne Particulate Matter PM2.5 from Mexico City Affects the Generation of Reactive Oxygen Species by Blood Neutrophils from Asthmatics: An In Vitro Approach. *J. Occup. Med. Toxicol.* **2009**, *4*, 17. [CrossRef] [PubMed]
48. Gobierno del Estado de Baja California. Programa Para Mejorar La Calidad Del Aire, de La Zona Metropolitana de Tijuana, Tecate, y Playas de Rosarito 2012–2020. 2011. Available online: https://www.gob.mx/cms/uploads/attachment/file/69288/9_ProAire_ZMT.pdf (accessed on 18 March 2020).
49. Takahama, S.; Russell, L.M.; Shores, C.A.; Marr, L.C.; Zheng, J.; Levy, M.; Zhang, R.; Castillo, E.; Rodriguez-ventura, J.G.; Quintana, P.J.E.; et al. Diesel Vehicle and Urban Burning Contributions to Black Carbon Concentrations and Size Distributions in Tijuana, Mexico, during the Cal-Mex 2010 Campaign. *Atmos. Environ.* **2014**, *88*, 341–352. [CrossRef]
50. Shores, C.A.; Klapmeyer, M.E.; Quadros, M.E.; Marr, L.C. Sources and Transport of Black Carbon at the California e Mexico Border. *Atmos. Environ.* **2013**, *70*, 490–499. [CrossRef]
51. Bei, N.; Li, G.; Zavala, M.; Barrera, H.; Torres, R.; Grutter, M.; Gutiérrez, W.; García, M.; Ruiz-Suarez, L.G.; Ortinez, A.; et al. Meteorological Overview and Plume Transport Patterns during Cal-Mex 2010. *Atmos. Environ.* **2013**, *70*, 477–489. [CrossRef]
52. Limon-Sanchez, M.T.; Carbajal-Romero, P.; Hernandez-Mena, L.; Saldarriaga-Norena, H.; Lopez-Lopez, A.; Cosio-Ramirez, R.; Arriaga-Colina, L.J.; Smith, W. Black Carbon in PM2.5, Data from Two Urban Sites in Guadalajara, Mexico during 2008. *Atmos. Pollut. Res.* **2011**, *2*, 358–365. [CrossRef]
53. Peralta, O.; Ortínez-Alvarez, A.; Basaldud, R.; Santiago, N.; Alvarez-Ospina, H.; de la Cruz, K.; Barrera, V.; de la Luz Espinosa, M.; Saavedra, I.; Castro, T.; et al. Atmospheric Black Carbon Concentrations in Mexico. *Atmos. Res.* **2019**, *230*, 104626. [CrossRef]
54. Liu, B.; He, M.M.; Wu, C.; Li, J.; Li, Y.; Lau, N.T.; Yu, J.Z.; Lau, A.K.H.; Fung, J.C.H.; Hoi, K.I.; et al. Potential Exposure to Fine Particulate Matter (PM2.5) and Black Carbon on Jogging Trails in Macau. *Atmos. Environ.* **2019**, *198*, 23–33. [CrossRef]
55. Liñán-Abanto, R.; Salcedo, D.; Castro, T.; Carabeli, G.; Peralta, O.; Arnott, P.; Ruiz Suárez, L.; Paredes Miranda, G. Mediciones Continuas de Carbono Negro, Monóxido de Carbono y Dióxido de Carbono, Durante La Temporada Seca Caliente 2016, En Un Sitio Periurbano de Querétaro, México. *Cienc. Desarro.* **2020**, *19*, 68–76. [CrossRef]
56. Şahin, Ü.A.; Onat, B.; Akın, Ö.; Ayvaz, C.; Uzun, B.; Mangır, N.; Doğan, M.; Harrison, R.M. Temporal Variations of Atmospheric Black Carbon and Its Relation to Other Pollutants and Meteorological Factors at an Urban Traffic Site in Istanbul. *Atmos. Pollut. Res.* **2020**, *11*, 1051–1062. [CrossRef]
57. Rocha Romero, D.; Orraca Romano, P.P. Estudiantes de Educación Superior Transfronterizos: Residir En México y Estudiar En Estados Unidos. *Front. Norte* **2018**, *30*, 103–128. [CrossRef]
58. US Environmental Protection Agency (US EPA). *Report to Congress on Black Carbon*; Department of the Interior, Environment, and Related Agencies Appropriations Act: Raleigh, NC, USA, 2012. Available online: https://19january2017snapshot.epa.gov/www3/airquality/blackcarbon/2012report/fullreport.pdf (accessed on 13 June 2020).
59. Tiwari, S.; Srivastava, A.K.; Bisht, D.S.; Parmita, P.; Srivastava, M.K.; Attri, S.D. Diurnal and Seasonal Variations of Black Carbon and PM2.5 over New Delhi, India: Influence of Meteorology. *Atmos. Res.* **2013**, *125–126*, 50–62. [CrossRef]
60. Gaitan, G.E.M.; Mancilla, Y.; Dom, A.M. Black Carbon-Organic Carbon and Black Carbon-PM2.5 Ratios of the Major Emissions Sources in the Monterrey, Mexico. Conference: 2° Congreso Interamericano de Cambio Climatico. 2016. Available online: https://www.researchgate.net/publication/298787121_Black_Carbon-Organic_Carbon_and_Black_Carbon-PM25_Ratios_of_the_Major_Emissions_Sources_in_Monterrey_Mexico (accessed on 11 March 2020).
61. Liu, Q.; Ma, T.; Olson, M.R.; Liu, Y.; Zhang, T.; Wu, Y.; Schauer, J.J. Temporal variations of black carbon during haze and non-haze days in Beijing. *Sci. Rep.* **2016**, *6*, 33331. [CrossRef] [PubMed]
62. Gao, D.; Mulholland, J.A.; Russell, A.G.; Weber, R.J. Characterization of water-insoluble oxidative potential of PM2.5 using the dithiothreitol assay. *Atmos. Environ.* **2020**, *224*, 117327. [CrossRef]
63. Shirmohammadi, F.; Hasheminassab, S.; Wang, D.; Schauer, J.J.; Shafer, M.M.; Delfino, R.J.; Sioutas, C. The relative importance of tailpipe and non-talpipe emissions on the oxidative potential of ambient particles in Los Angeles, CA. *Faraday Discuss.* **2016**, *189*, 361–380. [CrossRef] [PubMed]
64. Delfino, R.J.; Staimer, N.; Tjoa, T.; Gillen, S.L.; Schauer, J.J.; Shafer, M.M. Airway inflammation and oxidative potential of air pollutant particles in a pediatric asthma panel. *J. Expo. Sci. Environ. Epidemiol.* **2013**, *23*, 466–473. [CrossRef] [PubMed]
65. Cho, A.K.; Sioutas, C.; Miguel, A.H.; Kumagai, Y.; Schmitz, D.A.; Singh, M.; Eiguren-Fernandez, A.; Froines, J.R. Redox activity of airborne particulate matter at different sites in the Los Angeles Basin. *Environ. Res.* **2005**, *99*, 40–47. [CrossRef]
66. Shirmohammadi, F.; Wang, D.; Hasheminassab, S.; Verma, V.; Schauer, J.J.; Shafer, M.M.; Sioutas, C. Oxidative potential of on-road fine particulate matter (PM2.5) measured on major freeways of Los Angeles, CA, and a 10-year comparison with earlier roadside studies. *Atmos. Environ.* **2017**, *148*, 102–114. [CrossRef]
67. Madrigano, J.; Baccarelli, A.; Wright, R.O.; Suh, H.; Sparrow, D.; Vokonas, P.S.; Schwartz, J. Air pollution, obesity, genes and cellular adhesion molecules. *Occup. Environ. Med.* **2010**, *67*, 312–317. [CrossRef] [PubMed]
68. Velasco, E.; Retama, A.; Segovia, E.; Ramos, R. Particle exposure and inhaled dose while commuting by public transport in Mexico City. *Atmos. Environ.* **2019**, *219*, 117044. [CrossRef]

69. Alvarez-Pedrerol, M.; Rivas, I.; López-Vicente, M.; Suades-González, E.; Donaire-Gonzalez, D.; Cirach, M.; de Castro, M.; Esnaola, M.; Basagaña, X.; Dadvand, P.; et al. Impact of commuting exposure to traffic-related air pollution on cognitive development in children walking to school. *Environ. Pollut.* **2017**, *231*, 837–844. [CrossRef]
70. Zurita, R.; Quintana, P.J.E.; Toledano-Magaña, Y.; Wakida, F.T.; Montoya, L.D.; Castillo, J.E. Black carbon concentration at the major US-Mexico Port of Entry San Ysidro/El Chaparral. Mendeley Data 2020 V1. Available online: https://data.mendeley.com/datasets/3zb8vkpnyx/1 (accessed on 26 November 2020).